Fracture of Hardened Cement Paste and Concrete

Fariborz Radjy and Torben C. Hansen
Building Materials Laboratory
Technical University of Denmark

ABSTRACT

The paper reviews literature on work in the field of fracture mechanics of hardened cement paste, cement mortar and concrete from the very beginning in 1929. Application of Griffith's theory for fracture of brittle solids to heterogeneous composite cement and concrete materials is discussed. Experimental data on fracture parameters from previous work by others is tabulated and compared. Macroscopic fracture mechanism and crack patterns of cement paste and concrete in tension and compression, as well as microscopic aspects of fracture mechanism in cement paste, are discussed.

INTRODUCTION

Fracture mechanics concepts have proved invaluable tools in both characterizing and elucidating the failure processes in metals (1,2). Principles of fracture mechanics are also finding increasing applications in polymers (3) and ceramics (4,5). In the late 1940's and the early 1950's, the first systematic applications of fracture mechanics were made to metals. Applications to polymers and ceramics are of more recent origin, triggered to a large extent by the need to understand the behavior of an ever increasing, newer class of composite materials.

The first application of fracture mechanics to concrete was reported in 1961 by Kaplan (6). Since then, a dozen or so publications dealing with this matter have appeared. In the last decade or so, a parallel research effort has dealt with the process of microcracking in concrete and its relationship to the macroscopic stress-strain behavior, concentrating particularly on problems associated with the aggregate-matrix interaction (7-12). Insight gained into the processes of microcracking when viewed according to concepts of fracture mechanics has led to a qualitative understanding of the different fracture behavior of concrete in tension and compression (13), as well as elucidating (14, 15) the differences between the fracture behavior of concrete, mortar and hardened cement paste. Here, we consider application of fracture mechanics concepts to concrete systems both at the microscopic and the macroscopic levels. At the same time, a tabulation of fracture mechanics parameters reported by various investigators will be presented, and appraised.

FRACTURE THEORY

Theoretical strengths of solids are generally 10 to 10^3 times greater than observed values. In the Griffith-Irwin formulation of fracture mechanics (1,2,5), this is explained by existence of sharp 'cracks' or flaws in the material's structure. The original Griffith analysis is developed both from a stress and an energy point of view. It is concerned

with the stability of a crack in a very large, perfectly brittle and elastic plate subjected to tension (Fig. 1). According to the stress point of view, the crack will propagate when the tensile stresses at the tip of the crack reach the theoretical strength. Thus, the macroscopic fracture strength, σ_f, is given by (1, p.50) (2)

$$\sigma_f = \sqrt{\frac{E\gamma_s}{4c}\,\frac{\rho}{a_o}}\,, \qquad (1)$$

where

E = elasticity modulus
γ_s = surface energy
ρ = radius of curvature at the crack tip
c = half length of crack
a_o = equilibrium spacing between lattice planes in the absence of applied stresses.

Eq. 1 is, in part, attributed (5) to Orowan.

The energy analysis is concerned with the conversion of strain energy to surface energy. Consider an uncracked plate of unit thickness similar to Fig. 1, but held between fixed grips in a stressed condition. By introducing a crack of length 2c, a strain energy U is released (16):

$$U = \frac{\Pi\sigma^2 c^2}{E}\,, \text{ plane stress,} \qquad (2)$$

Now impose a virtual extension on the crack by the amount δc. The corresponding release in the strain energy is $\delta U = 2\Pi\sigma^2 c\cdot\delta c/E$. At the same time the surface energy of the system has increased by an amount $\delta T = 4\gamma_s\cdot\delta c$. Griffith postulates instability if $\delta U \geq \delta T$, that is to say when the virtual release of strain energy exceeds the virtual increase of surface energy. Thus, the macroscopic fracture stress in plane stress is given by

$$\sigma_f = \sqrt{\frac{2\gamma_s E}{\Pi c}}\,. \qquad (3)$$

The σ_f-values given by Eqs. 1 and 3 are equal if $\rho = 8a_o/\pi \simeq 3a_o$. This has been interpreted (1, p.56) as indicating that the radius of a propagating crack in a perfectly brittle solid should be $\sim 3a_o$. One may wonder how this condition can ever be attained for a microporous solid such as hardened cement paste, even when considered perfectly brittle.

The Griffith analysis was developed for a crack in a plate of infinite extension, and crack propagation was assumed to be perfectly brittle. The Griffith analysis has been generalized for application to specimens of finite dimensions, and for application to cases in which crack propagation is accompanied by plastic (or viscous) deformation. These generalizations have been made by Irwin and Orowan, but notably Irwin (5). Analogous to the Griffith method, the Griffith-Irwin analysis involves both an energy and a stress method. In the stress method, instead of postulating that the tensile stresses at the tip of the crack reach a critical value, the fracture criterion is formulated in terms of a critical value, K_c, for the stress intensity factor K:

$$K \geqslant K_c, \tag{4}$$

where K_c is a material constant. The significance of K is that it specifies the entire stress and displacement field in the vicinity of the crack tip. The stress intensity factor has the general form $K = \alpha S$, where α is a geometric factor and S is the applied load. Because K is linear in S, its value in a complicated situation may be derived by the superposition principle.

The energy method is developed in terms of the strain energy release rate G. Referring to Fig. 1, the area A of the crack when considered as a line is $A = 2c$. Thus, for a virtual extension: $\delta A = 2\delta c$, and G is defined as

$$G = \frac{dU}{dA}. \tag{5}$$

Because G equals the differential of an energy tending to

advance the crack with respect to its conjugate displacement, crack extension, G is also referred to as the 'crack extension force'. The fracture criterion is now stated as

$$G \geqslant G_c, \tag{6}$$

where the 'toughness' G_c is a material constant. The criteria of Eqs. 4 and 6 are not independent, for it is found that (5)

$$G = \frac{K^2}{E}, \text{ plane stress.} \tag{7}$$

Eq. 7 applies also for the case where $G = G_c$ and $K = K_c$.

Application of Eq. 6 to the case of the infinite plate (use Eqs. 2 and 5) leads to

$$\sigma_f = \sqrt{\frac{G_c E}{\pi c}}, \text{ plane stress.} \tag{8}$$

By comparing Eqs. 3 and 8 we obtain $G_c = 2\gamma_s$ for a perfectly brittle solid. Analogously, a generalized fracture surface energy is defined by

$$\gamma_f = G_c/2. \tag{9}$$

For the case where, for instance, plastic deformation in the immediate vicinity of the crack is important, $\gamma_f = \gamma_s + \gamma_p$. That is, the strain energy released is used both for the creation of new surfaces and plastic work.

Even though for the majority of engineering materials $\gamma_f >> \gamma_s$, the magnitude of the surface energy γ_s is of considerable interest since it serves as a norm against which the extent of brittleness can be measured. Thus, the ratio γ_f/γ_s increases from its minimum value of unity as the material becomes more brittle. Table 1 lists γ_f and γ_s for a few materials for conditions under which the fracture is apparently brittle. Although the steel specimen is tested below its ductile-brittle transition temperature, and the PMMA sample is

far below its glass transition temperature (T_g = 105°C), the γ_f values are some orders of magnitude larger than γ_s. In contradistinction, for the glass and the hardened cement paste specimens the ratio γ_f/γ_s is not too large. On a relative scale, therefore, hardened cement paste is much more like glass than a glassy polymer or a brittle steel in its fracture behavior. The brittleness of hardened cement paste becomes even more evident when considering that $\gamma_f/\gamma_s \simeq 10^5$ for a ductile metal such as copper.

FRACTURE TESTING

The aim of fracture testing is to evaluate the parameters G_c, K_c and γ_f. The subject has been well reviewed by Wiederhorn (5), and discussed in some detail in various ASTM publications such as Ref. (20). Here, only the mere outlines will be mentioned.

There are three experimental methods currently prevalent: a) the analytic method; b) the compliance method; c) the slow bend test.

In method (a) a test geometry is chosen for which an analytical expression for K is available. The specimen is loaded to fracture, the failure load P_f noted, and K_c is calculated by evaluating K at $P = P_f$.

In method (b) the compliance λ (inverse of modulus) of specimens of given geometry and known crack lengths, are measured as a function of the crack length c. Using this information, G_c is then evaluated from a general equation (independent of size and geometry) which relates G to the load P and $(\partial\lambda/\partial c)_P$.

In the 'slow bend test', the specimen is slowly loaded in flexure in a suitable, stiff testing machine such that the complete load deflection curve to failure can be generated, Fig. 2. The fracture surface energy γ_f is obtained by dividing the total work to fracture (area under load-deformation curve) by the fracture surface area. It is important to ensure that there is no contribution to the strain energy released at fracture from the testing machine (14, 21).

FRACTURE OF HARDENED CEMENT PASTE

The fracture parameters γ_f and K_c obtained by various investigators for hardened cement paste are listed in Table 2. Moavenzadeh and Kuguel (14) measured γ_f by the slow bend method, as well as two different analytical methods. They found that γ_f (slow bend) was consistently larger than γ_f (analytical), Table 2. They attribute this difference to the difficulty of attaining a sufficiently slow fracture. It appears, therefore, that γ_f (analytical) should be more reliable. The analytical method, however, suffers from the possibility of slow crack growth prior to fracture. Cooper and Figg (23) used double triangularly side notched beams (apex on tension side) in order to specifically attain a slow bend condition. However, judging from the relative magnitude of their results (Table 2, lines 5 and 6), they have considerably overestimated γ_f. Shah and McGarry (15) also report toughness (G_c) values (converted to γ_f in Table 2, lines 7-8) obtained by the slow bend test. Their results show that as the notch depth increases, γ_f decreases rapidly. However, at the same c/d (c = notch depth, d = beam depth) ratio their result compares favorably with that of Moavenzadeh and Kuguel (14), cf. lines 1 and 8 of Table 2. Naus and Lott (22) report only 'fracture toughness' (K_c) values. They also varied the notch depth (in contrast to others, introduced by a teflon coated fiber glass cloth), but do not discuss the effect of this parameter. Their K_c-value compares well with that of Moavenzadeh and Kuguel (14), Table 2 (lines 2 and 4). The results discussed so far have been obtained either in single point or three point bending. Chau and Patterson (24) report $\gamma_f \simeq 0.5 \times 10^3$ erg/cm^2, obtained by the analytic method in pure tension for a high aluminia cement of w/c = 0.4 and age = 9 days.

Other general observations are: 1) fracture occurs by a single, straigth crack (14); 2) K_c decreases significantly with both increasing water/cement ratio and entrained air content (22); 3) except at possibly very early ages, the fracture parameters are relatively insensitive to the duration of curing period (22); 4) the magnitude of proper values for the fracture parameters are uncertain, but at a w/c = 0.5 and age = 28 days

the probable orders of magnitude are $\gamma_f \simeq 2 \times 10^3$, $G_c \simeq 10^3$ ergs/cm^2 and $K_c \simeq 10^7$ dyne cm$^{-2/3}$.

The fracture process in terms of some of the prevalent views of the microstructure has been analyzed elsewhere (25). The analysis in (25) considers the effect of porosity on σ_f and addresses the question: 'how should γ_f be interpreted and what is its limiting value in case of perfect brittleness?'.

On the microscopic level the fracture process is viewed in terms of two limiting, alternative assumptions. According to the first of these two alternative views it is assumed that all the gel particles encountered by the crack front break . Then, it is found that the assumption γ_f (brittle) $\simeq$ γ_s (tobermorite) is justifiable.

According to the second of the two limiting views, the assumption is made that no gel particles break and the fracture proceeds solely along the internal surface of hardened cement paste. This second model is prompted by the fact that the gel particles are very small (~ 1 μm long) and, therefore, may exhibit whisker-like strength. The fracture stress is now given by

$$\sigma_f \simeq (1 - \varepsilon)^2 \sqrt{\frac{2 \cdot \delta \cdot \Omega \cdot \gamma_f^* \cdot E_o}{\pi c}} , \qquad (10)$$

where δ is the width of the fracture zone (a region where all the internal surface is bared by the fracture process), Ω (cm^2/cm^3) is the specific surface of the gel particles, and γ_f^* is the 'intrinsic' or 'microscopic' surface energy of fracture. The factor $\delta\Omega$ is a microscopic tortuosity factor which is shown to be of the order of 5. γ_f^* has, in general, contributions from surface forces, chemical and hydrogen bonds and inelastic processes. The value of γ_f^* for the case of perfect brittleness and in the absence of chemical and hydrogen bonds, is found to be of the order of $\gamma_s/10$ to $\gamma_s/100$ -- 4 to 40 ergs/cm^2 -- where γ_s is the surface energy of tobermorite. Accordingly, γ_f^* (measured)/γ_f^*(brittle) $\simeq$ 10 to 100 which is at least an order of magnitude larger than when the assumption is made that γ_f (brittle) $\simeq$ γ_s(tobermorite).

The point of this analysis, apart from interpreting γ_f, is that the value of γ_f(brittle) used in obtaining the γ_f(observed)/γ_f(brittle) ratio as a measure of relative brittleness, is very much a function of the microscopic processes responsible for fracture; to compare γ_f(observed) with γ_s(tobermorite) is not, necessarily, relevant.

The above analysis, apart from its obvious oversimplifications, also involves the fundamental assumption that hardened cement paste is a homogeneous material. Since, in general, there is always a significant content of calcium hydroxide, and possibly unhydrated grains, the assumption of homogeneity is not reasonable, and the possible role of both calcium hydroxide and clinker grains must be considered when interpreting experimental data. The elegant study by Berger (26) using optical microscopy is particularly relevant in this respect. As seen in Fig. 3 , for instance, the crack tends to go around, rather than through the calcium hydroxide crystals. These crystals elevate tortuosity of fracture.

FRACTURE OF MORTAR AND CONCRETE

Table 3 lists the effective fracture parameter γ_f' and K_c' reported by various investigators for mortar and concrete. It is necessary to refer to 'effective' parameters for two reasons: firstly, the fracture surface area is generally considerably in excess of the nominal area of the fracture; secondly, both mortar and concrete being composites, even on a macro scale, there is some doubt as to the precise significance of γ_f and K_c in such a context.

The experimental observations may be summarized as follows: 1) at the same w/c ratio, the value of the fracture parameters for mortar and concrete are significantly higher than the corresponding values for hardened cement paste (Fig. 2); 2) for mortars, beyond ~50% sand content, the parameter K_c' is relatively insensitive to the content of sand (22, 28); 3) increasing w/c ratio, decreases K_c' for mortars (22) while the K_c' of concrete remains unchanged (22, 28); 4) the curing period has a significant effect on K_c' for concrete, while K_c' (mortar)

is not as sensitive to the curing time (22); 5) the content of coarse aggregate is the most important concrete parameter: as the amount of aggregate increases, so does γ_f' and K_c' (6,14, 15, 22, 28, 29).

In the case of mortars and concretes, the crack generally goes around the sand and aggregate particles, thus increasing the actual area of fracture by a factor of the order of 2 for mortars (14). For concrete, furthermore, it is found that extensive side cracking or microcracking occurs (14,15). The actual area of the fracture can be as high as 10 times the nominal area of fracture (14). This excess surface area of fracture, then, is a partial reason why the γ_f'-values in Table 3 are considerably higher than the γ_f-values for hardened cement paste in Table 2: The hard sand or aggregate particles deviate the crack from a straight line making its path more tortuous and, therefore, its energy demand more severe.

There is some disagreement regarding the effect of the notch size on the value of γ_f' and K_c'. Shah and McGarry (15) find that as the c/d ratio increases, γ_f' and K_c' decrease rapidly, Kaplan (6), Naus and Lott (22) and Lott and Kesler (28), however, find that the fracture parameters are independent of c/d. Harris et.al. (30) measured γ_f' (mortar) for beams of c/d = 0.1 to 0.6. They found that beyond a c/d of 0.3 the results were relatively insensitive to the notch depth. In metals too the test geometry can have a considerable influence on the results, and a major effort has been made in order to arrive at some reasonable standards (20). A similar effort in the case of concrete is needed.

Because the fracture parameters are measured with the implicit assumption that the material is homogeneous, Lott and Kesler (28) refer to K_c' as a 'pseudo-fracture toughness' and write

$$K_c' = K_c(\text{hcp})^{*} + f(\text{ARR}), \qquad (11)$$

where f(ARR) is an arresting function (with respect to crack propagation), reflecting the heterogeneous nature of concrete, and depending on the properties of both the matrix and the aggregate. Shah and McGarry (15) have suggested that for con-

*hcp = hardened cement paste

crete made with normal aggregate, debonding or bond cracking is a predominant crack arresting mechanism. These suggestions are particularly plausible since studies (10,11,31,32) of the aggregate-matrix interface show that this region is generally weaker than the matrix, as well as being the source of flaws due to bleeding and, probably, containing cracks even prior to loading. On the other hand, since stress analysis (8,12) has shown that this region also contains localities of high stress concentration, the flaws at the aggregate-matrix interface become even more critical and make debonding even easier. Apart from such qualitative explanations, no quantitative, theoretical relationships for the effect of aggregate on the fracture parameters have been given. It appears, however, that at least one aspect of the dependence of K_c' and G_c' (= $2\gamma_f'$) on the aggregate content is tractable. According to Eq. 7, K_c' and G_c' are interrelated through E. Now, the dependence of E on aggregate content has been formulated through the application of the composite theory (33,34), making one of the influences of the aggregate phase potentially apparent. Apart from this semi-emperical extension, however, not much else can be said before the stress intensity factor for a notch in whose vicinity aggregate particles are allowed, is obtained.

The most common mode of strength testing in concrete technology is in compression. Yet, all the discussion so far has been concerned with crack propagation in a tensile stress field. Furthermore, macroscopic failure criteria, such as the 'Mohr-Coulomb' criterion, have been applied (7,12) to concrete under various states of loading quite successfully. What, then, is the connection between the fracture parameters discussed and the failure load in more realistic, engineering situations, and how can the Griffith view -- the "flaw" concept -- be correlated with macroscopic criteria? Griffith in 1924 (35) performed an analysis which achieved just such a conciliation,

and led to what is now known as the "Griffith criterion". Glucklich (13) appears to be the first to have applied this criterion to the compressive failure of concrete.

Following Paul (35), consider a plate in a state of biaxial stress, and let it contain a large number of randomly oriented microcracks, with a given crack as shown in Fig. 4. For each set of values (P,Q) there is one orientation χ (critical) for which the tensile stress at the crack tip is more than any other orientation. If (P, Q) are at the critical level (on the failure envelope), then this critical crack could propagate and cause fracture. Detailed analysis leads to the failure envelope shown in Fig. 4 , and for Q > P is given by

$$\left.\begin{aligned} &P = S_t, \quad \text{if } (3P + Q) < 0, \\ &(P - Q)^2 - 8S_t(P + Q) = 0, \quad \text{if } 3P + Q > 0, \\ &\cos 2\chi_{cr} = \frac{Q - P}{2(Q + P)}. \end{aligned}\right\} \qquad (12)$$

The sign convention adopted in Eqs. 12 is that compression is positive. The quantity S_t is the tensile strength (a negative number). An interesting prediction,and at the same time an apparent limitation of this theory is that the compressive strength is eight times the tensile strength. Although the measured values of S_c/S_t for many materials are close to 8, there are also significant deviations ($S_c/S_t \simeq 10$ for concrete). Paul and Gangal (35) have further developed this theory to account for this apparent discrepancy. The most critical crack (Fig. 5) becomes unstable by the developing "braching cracks". The tendency for these branching cracks is to turn into a direction parallel to the applied compressive load; thus becoming immobilized. Now, the second most critical flaw becomes unstable, develops branching cracks, etc. Each flaw (given initial inclination) will have a failure envelop associated with it, and as the most severe flaws develop branching cracks, a process of "fracture hardening" will occur (Fig. 6) until enough cracks have developed that the material

will disintegrate. As noted by Glucklich (13), the most important characteristic of this sort of compressive fracture is that it occurs by slow, stable crack growth: an ever increasing load is needed for crack propagation. The most important factor in this respect appears to be the progressive development of microcracks in concrete as described in the following.

On the basis of observation of volumetric changes of plain concrete cylinders in concentric compression Brandtzaeg and co-workers (36) in 1929 were the first to suggest that failure of concrete progresses by internal splitting in microscopic regions distributed throughout the material. In 1950 Berg (37) observed tiny cracks developing in the direction of applied load on concrete specimens loaded in compression. In 1952 Jones (38) found a change in the sonic velocity through concrete loaded to 25-30 percent of the ultimate load, which indicated the formation of internal microscopic flaws or cracks in the material. In 1958 Hansen (39) demonstrated that formation of small cracks in the concrete structure is correlated with non-linearity of the stress-strain curve of concrete.

Using an X-ray technique Slate and Olsefski (40) showed that flaws or microcracks exist in the bond phase between cement mortar and aggregate of concrete even before any loading. Using the same technique this conclusion was later confirmed by Robinson (41) and Nielsen (9) among others. Hsu, Slate and others (42) also used a different technique in order to observe microcracking. A smooth plane section through the specimen was cut. The cracks were filled with red dye, and the cross-section was examined under a microscope. Ash (32) demonstrated that some of these flaws which exist in concrete specimens before loading are formed during casting of the concrete due to bleeding. Hsu (43) showed that some flaws or microcracks may form due to development of tensile stresses in the cement mortar phase, when the mortar shrinks around restraining, hard aggregate particles during later drying. The flaws or microcracks in the bond phase which exist in concrete before any loading require very large microscopic magnification in order to be seen without any use of special techniques. In the case of flaws which are formed due to bleeding Ash (32) found that they were areas of high porosity

and low strength in the bond phase, but that no gap existed between aggregate particles or mortar. However, there can be no doubt that preexisting flaws in the bond phase may serve as crack initiators in concrete.

Applying an analysis first presented by Goodier (44) of the stress distribution around a single elastic particle located in a continuous elastic matrix of infinite extension and submitted to a uniaxial compressive stress, Hansen (8) showed that tensile stresses develop in concrete in the bond phase between aggregate particles and cement mortar perpendicular to the direction of applied load. In addition it was shown experimentally that the first bond cracks develop on the side of large aggregate particles corresponding to the location of maximum tensile stresses when concrete specimens are loaded to about half the compressive strength of the concrete. These cracks are easily observed in a light-microscope under low magnification. They are orders of magnitude larger than the pre-existing flaws or microcracks mentioned earlier, but are probably initiated by these flaws. The cracks propagate through the cement mortar matrix to other aggregate particles as load is increased (see Fig. 7) and they ultimately cause the specimens to fail. It was also shown that fracture of concrete under sustained and pulsating load is due to gradual growth of the same type of cracks.

Using the finite element analysis Buyukozturk, Nilson and Slate (12) made a more accurate analysis of the deformation and failure behavior of a composite model of concrete in plane uniaxial compressive stress. The model was composed of a matrix in which were embedded nine circular discs of equal size in a rectangular array. This analysis accounts for the influence of non-homogeneity, models interfacial behavior, and includes recognition of interface debonding and resulting progressive fracture. The analysis revealed that formation of bond cracks is due to shear stresses as well as tensile stresses. This analysis and the corresponding experiments confirmed earlier observations by Hansen but in addition they do provide a much better understanding of the effect of non-homogeneities and the interfacial behavior of systems of aggregate particles in general (see Fig. 8). It should be mentioned though that the fact that the macroscopic failure en-

velope conforms to the Coulomb-Mohr theory as used by Buyukozturk et.al. (12) does not necessarily mean that fracture is partially by shear as concluded by the authors. Newman (7) and Paul (35) have shown that the Coulomb-Mohr theory with tension cutoffs agrees qualitatively with the Griffith theory discussed previously (see Fig. 4), which is based entirely on tensile failure.

Finally the work of Paul and Gangal (35) should be mentioned, which provides an elegant explanation of the hourglass type of failure observed in concrete when lateral expansion is restrained at the platens of the testing machine.

TABLE 1
Comparison of True (γ_s) and Fracture (γ_f) Surface Energies

	γ_s ergs/cm^2	γ_f Ref. ergs/cm^2	Ref.	γ_f/γ_s
Mild Steel (-150°C)	2×10^3	(17) 4×10^6	(1,p.74)	2×10^3
PMMA (-46°C)	500	(17) 2×10^5	(18)	4×10^2
Silica Glass	1.2×10^3	(17) 3×10^3	(1,p.597)	2.5
Hardened Cement Paste *	400	(19) 2.3×10^3	(14)	~6

*
γ_s assumed equal to the surface energy of tobermorite gel.
$\gamma_f = G_c/2$ value from Ref. (14), Table 3, 28 days cured specimen with w/c = 0.5.

PL IX-133

$\gamma_f = 10^3$(ergs/cm^2), $K_c = 10^7$(dynes.cm$^{-3/2}$)

Material	w/c	Age	Test Condition	Slow Bend γ_f	Slow Bend K_c	Analytical γ_f	Analytical K_c	Specimen[a] Geometry cms.	Ref.
Type I Portland cement	0.5	7 days	wet?	3.9	-	-	-	2.5x2.5x30,1	(14)
"	0.5	28 days	wet?	4.2	-	2.3 3.1	1.7	"	
"	0.35	28 days?	wet?	-	-	-	3.3	5x5x36,0.6-2.5	(22)
	[0.5][b]	"	"	-	-	-	[1.1]	"	(22)
Portland Cement	0.5	28 days	wet	12.4	-	-	-	2.5x5x20, double	(23)
"	0.5	"	dried in lab.air	14.9	-	-	-	side triangle	(23)
Type III Portland	0.54	6 days	wet	9.3	-	-	-	5x5x55,0.6	(15)
"	0.54	6 days	wet	3.9	-	-	-	5x5x55,1.9	(15)
"	"	"	"	2.6	-	-	-	5x5x55,2.5	(15)

[a] Depth x Breath x Length, Notch depth

[b] [ ] = Extrapolated

TABLE 3

Fracture Parameters for Mortar and Concrete

γ_f' and K_c' units as in Table 2

	Composition c:s:g:w†	Age	Test Condition	Slow Bend γ_f'	Slow Bend K_c'	Analytical γ_f'	Analytical K_c'	Loading	c/d*	Ref.
1)	1:2.4:0:0.5	28 days	wet	-	-	9.7	7.4	bending	0.17 -0.50	(6)
2)	1:2.4:2.7:0.5	"	"	-	-	10.8	9.1	"	"	"
3)	concrete?	?	?	-	-	2.6-6	-	tension	0.06 -0.37	(27)
4)	1:2.9:0:0.5	28 days	50% humidity	-	-	-	3.3	bending	0.125-0.375	(28)
5)	1:2.9:3.0:0.5	"	"	-	-	-	4.05	"	"	"
6)	1:?:0:0.5	28 days?	wet?	-	-	-	4.7	bending	0.125-0.5	(22)
7)	1:?:?:0.5	"	"	-	-	-	6.6	bending	0.125-0.375	(22)
8)	1:2:0:0.5	6 days	wet	25.2-12.8	-	-	-	bending	0.125-0.5	(15)
9)	1:1:1:0.5	"	"	36.7-14.9	-	-	-	"	"	"
10)	1:4:0:0.5	28 days	wet?	10.5	-	-	-	bending	0.4	(14,29)
11)	1:1.7:2.3:0.5	28 days	"	26.2	-	4.8	2.5	"	"	(14,29)
12)	1:3:0:0.67	28 days	wet	-	-	25	4.1	"	0.33	(30)

†cement:sand:gravel:water

*notch depth/beam depth or notch width/plate width ratio

REFERENCES

1. A.S. Tetelman and A.J. McEvily, Fracture of Structural Materials, Wiley, New York (1967)
2. W.W. Gerberich, J. Materials Science, 5, 283 (1970)
3. R.P. Kambour, I&EC Products Research & Development 11, 140 (1972)
4. R.W. Davidge and A.G. Evans, Mater.Sci.Eng. 6, 281 (1970)
5. S.M. Wiederhorn, in Mechanical and Thermal Properties of Ceramics: Proceedings of a Symposium April 1-2, 1968, p. 217. National Bureau of Standards, SP303, Washington, D.C. (1969)
6. M.F. Kaplan, J.ACI, 591 November (1961)
7. K. Newman, The Structure of Concrete and Its Behaviour Under Load, Proceedings of an International Conference, London, 1965, p.255. Cement and Concrete Association, London (1968)
8. T.C. Hansen, Paper No. 3 in ACI SP-20, Detroit, Mich., 43 (1968)
9. K.E.C. Nielsen, Aggregate Stresses in Concrete, Handlinger No. 41, Stockholm (1971)
10. S.P. Shah, Structure, Solid Mechanics and Engineering Design I, The Proceedings of the Southampton 1969 Civil Engineering Materials Conference, p.367. Wiley-Interscience, London (1971)
11. N. Swamy, Ref. (10), p.301
12. O. Buyukozturk, A.H. Nilson and F.O. Slate, J. Eng. Mechanics Div., Proc. ASCE, EM3, 98, 581 (1972)
13. J. Glucklich, J.Eng. Mechanics Div., Proc. ASCE. EM6, December, 127 (1963)
14. F. Moavenzadeh and R. Kuguel, J. Materials, JMLSA 4, no. 3, 497 (1969)
15. S.P. Shah and F.J. McGarry, J. Eng. Mechanics Div., Proc. ASCE, EM6, 97, December, 1663 (1971)
16. J.N. Goodier, Fracture II, H. Liebowitz (ed.), p.l. Academic Press (1968)

17. B.L. Averbach, Fracture I, H. Liebowitz (ed.), p.441. Academic Press (1968)
18. A.T. Dibenedetto and K.L. Trachte, J.Appl.Polymer Science 14, 2249 (1970)
19. D.L. Kantro, C.H. Weise and S. Brunauer, Symposium on Structure of Portland Cement Paste and Concrete, Highway Research Board Special Report No. 90, p.309. HRB, Washington, D.C. (1966). Also: PCA, Research Department, Bulletin 209
20. W.F. Brown, Jr. (ed.), Review of Developments in Plane Strain Fracture Toughness Testing, ASTM, STP 463, ASTM, Philadelphia (1970)
21. E.T. Brown, J.A. Hudson and M.S. Marathe, J.Eng.Mechanics Div., Proc. of ASCE, EM5, October, 1310 (1972)
22. D.J. Naus and J.L. Lott, ACI Journal, June, 481 (1969)
23. G.A. Cooper and J. Figg, Trans. Brit. Cer. Soc. 71, No. 1, 1 (1972)
24. H.C. Chau and W.A. Patterson, J. Materials Science 7, 856, (1972)
25. F. Radjy, Fracture of Hardened Cement Paste in relation to Surface Forces and Porosity, J.Am.Soc., submitted (1973)
26. R.L. Berger, Science 175, 626 (1972)
27. J.P. Romualdi and G.B. Batson, J.Eng. Mechanics Div., Proc. ASCE, EM3, June, 147 (1963)
28. J. Lott and C.E. Kesler, Ref. (19), p.204
29. F. Moavenzadeh, R. Kuguel and L.B. Keat, Fracture of Concrete, Research Report R68-5, Dept. of Civil Engr., MIT, Massachusetts (1968)
30. B. Harris, J. Varlow and C.D. Ellis, Cement and Concrete Research 2, 447 (1972)
31. S.P. Shah and F.O. Slate, Ref. (7), p.82
32. J.E. Ash, ACI Journal, April, 209 (1972)
33. T.C. Hansen, Ref. (7), p. 16
34. M. Te'eni, Ref.(10), p. 621
35. B. Paul, Ref. (16), p. 426

36. F.E. Richart, A. Brandtzaeg and L. Brown, University of Illinois Engineering Experiment Station, Bulletin 185, Urbana, April, (1929), p.102
37. O.J. Berg, Dokl. Acad. Nank. SSSR, Vol. 70, No. 4, p.617, (1950)
38. R. Jones, British Journal of Applied Physics, Vol. 3, No.7, July (1952), p.229-232
39. T.C. Hansen, Swedish Cement and Concrete Research Institute, Bul. 33, Stockholm (1958)
40. F.O. Slate and S. Olsefski, Journal of the American Concrete Institute, Proc. Vol. 60, No. 5, May (1963), p.575-588
41. G.S. Robinson, Proc. International Conference on Structure of Concrete, London (1965)
42. T.T.C. Hsu, F.O. Slate, G.M. Sturman and G. Winter, Journal of the American Concrete Institute, Proc. Vol. 60, No. 2, February (1963)
43. T.T.C. Hsu, Journal of the American Concrete Institute, Proc. Vol. 60, No. 3, March (1963), p.371-390
44. J.N. Goodier, Journal of Applied Mechanics, Vol. 55, (1933), p.39-44

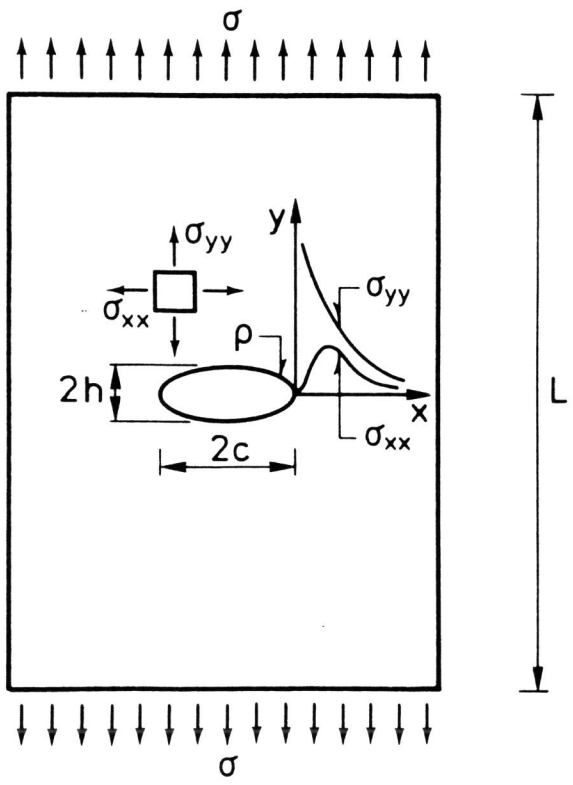

Fig. (1) Crack represented as an elliptical hole in a plate. The stress field in the vicinity of the crack tip is shown schematically.

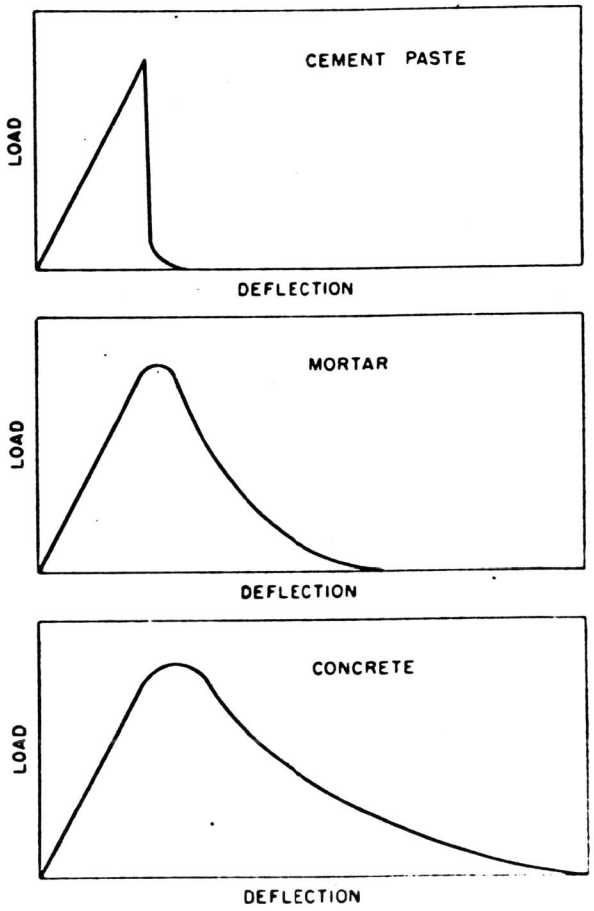

Fig. (2) Load-deflection curves for cement, mortar and concrete in slow-bend. After Moavenzadeh and Kuguel (14).

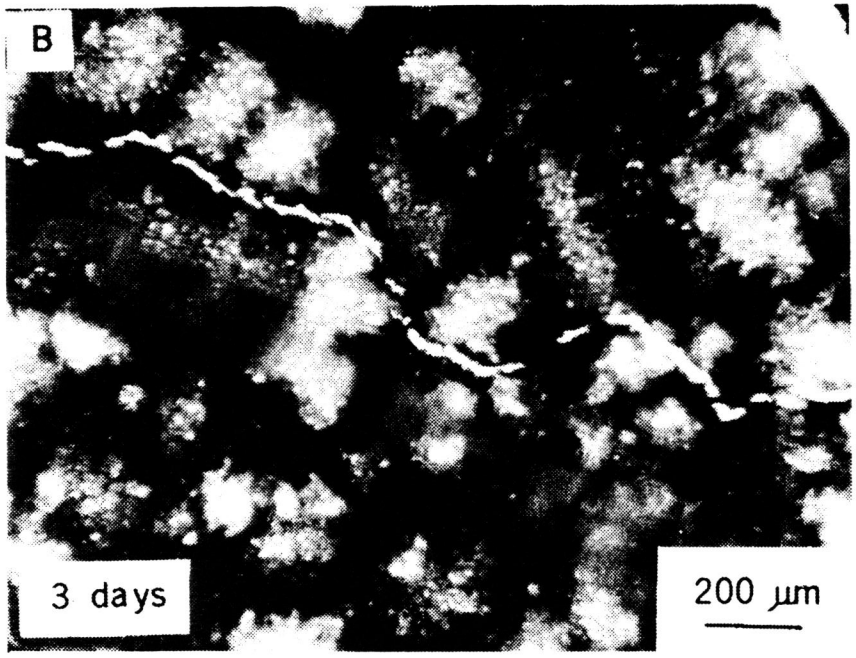

Fig. (3) Crack tortuosity in hardened cement paste due to calcium hydroxide crystals. After Berger (26).

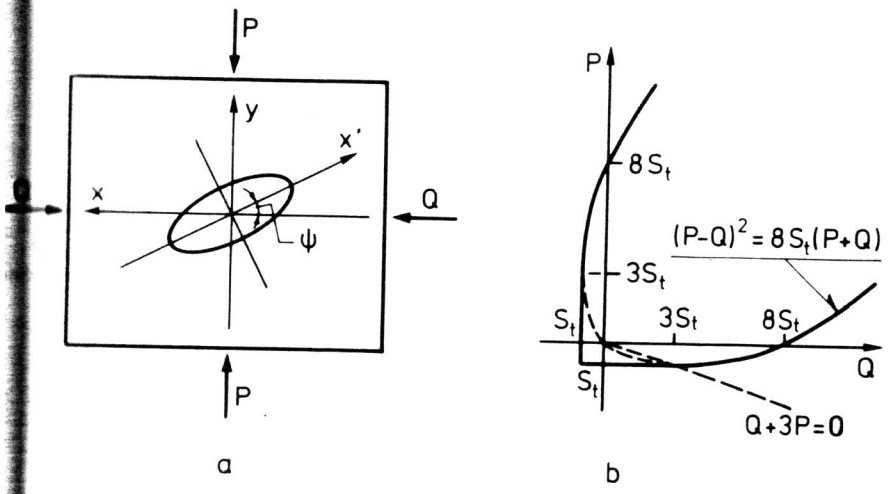

Fig. (4) (a) Elliptical crack and coordinate axis; (b) Griffith's criterion for fracture under biaxial principal stresses P and Q (compression considered positive). After Paul (35).

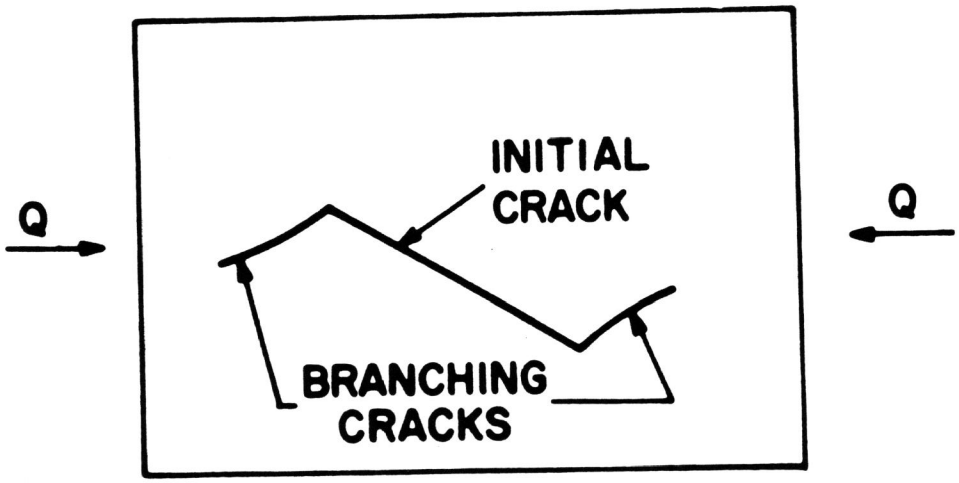

Fig. (5) Branching cracks observed in brittle plastic. After Brace and Bombolakis, from Paul (35).

PL IX-133

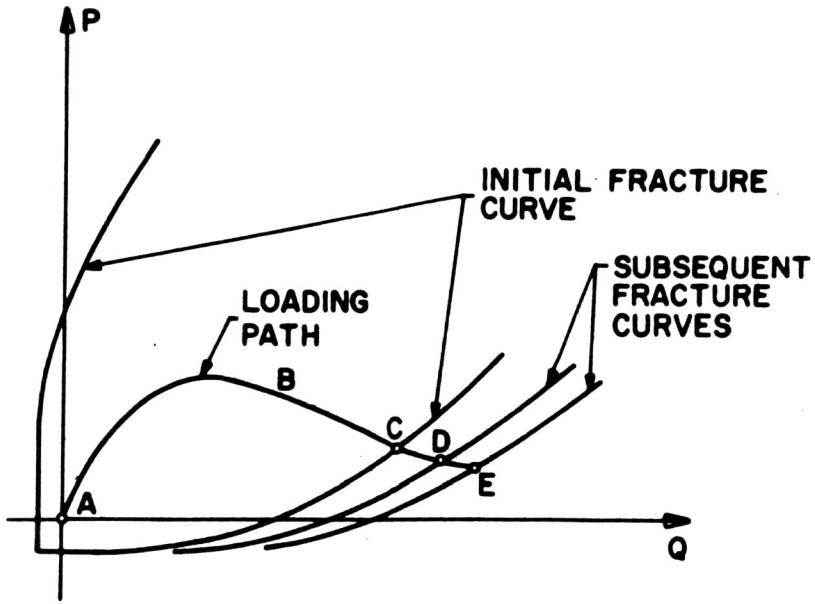

Fig. (6) Fracture hardening in a brittle material. As the most critical flaws develop branching cracks and become immobilized, the failure envelope shifts to higher stresses. After Paul (35).

PL IX-133

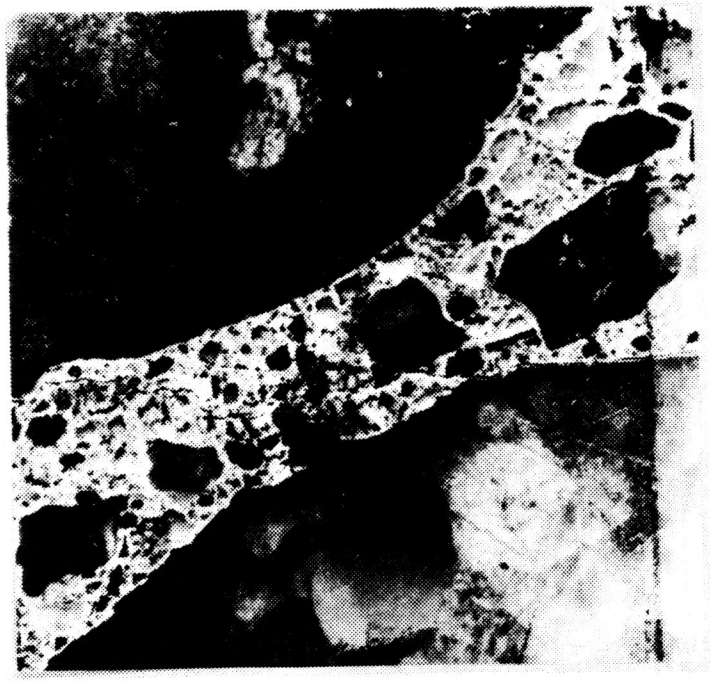

Fig. (7) Bond crack in concrete parallel to the direction of applied load at upper particle is seen to transverse the mortar phase to join a bond crack at lower particle (from ref. (8)).

PL IX-133

Fig. (8) Crack pattern in a model concrete subjected to uniaxial compression. Cracks develop parallel to the direction of applied load. After Buykozturk et.al (12).